Journal of Nonlinear Optical Physics & Materials
Vol. 27, No. 4 (2018) 1850047 (21 pages)

DOI: 10.1142/S0218863518500479

The manipulation of second-order nonlinear harmonic wave by structured material and structured light

Haigang Liu and Xianfeng Chen*

State Key Laboratory of Advanced Optical Communication Systems and Networks, School of Physics and Astronomy, Shanghai Jiao Tong University, Shanghai 200240, P. R. China

Key Laboratory for Laser plasma (Ministry of Education), Collaborative Innovation Center of IFSA (CICIFSA), Shanghai Jiao Tong University, Shanghai 200240, P. R. China
**xfchen@sjtu.edu.cn*

Accepted 13 December 2018
Published 4 February 2019

Nonlinear frequency conversion is the important method to get coherent radiation in all-optical waveband. The intentional manipulation of nonlinear harmonic wave, which has some special phase, amplitude, polarization, and so on, is also important to realize all kinds of optical micro-manipulation, optical micro-fabrication, and optical communication in all-optical waveband. There are three methods to manipulate such nonlinear harmonic wave, which are tailoring the functional facet, the structure of crystals, and the structure of the incident light. In this review, we will systematically introduce the fundamental principle and latest advances in this field and summarize the respective characteristics of these three methods.

Keywords: Nonlinear optics; diffractive optics; harmonic generation and mixing.

1. Introduction

2018 Nobel Prize in Physics was awarded to Arthur Ashkin, Gérard Mourou, and Donna Strickland for their "inventions in the field of laser physics", which are "optical tweezers" technique for manipulating small objects and "Chirped Pulse Amplification, CPA" technique for generating high-intensity, ultra-short optical pulses. It brings people's attention back to the property of the light wave and its application. Light wave with special phase, amplitude, and polarization distribution, such as Bessel beam, vortex beam, airy beam, vector beam, and so on, are important in the fields of optical micro-manipulation,[1–3] optical micro-fabrication,[4] optical imaging,[5,6] quantum optics,[7–10] and optical communication.[11–13] To get light wave with such special parameters, intentional wave-front controlling is needed. In linear optics, wave-front controlling technique is becoming increasingly sophisticated,

which has been used to realize arbitrary parameters' manipulation.[14] In recent years, wave-front shaping of a nonlinear harmonic wave has attracted more and more interest. The manipulation of nonlinear harmonic wave would make it possible to generate in all-optical waveband. It will extremely promote the optical micro-manipulation, optical micro-fabrication, optical imaging, and optical communication in the all-optical scope.

The manipulation of nonlinear harmonic wave relates to two processes, which are the generation process and the manipulation process. Intuitively, there are three methods to manipulate such nonlinear harmonics wave according to the sequence of generation and manipulation. The first method can be treated as the linear method, in which the first step is the generation of nonlinear harmonics wave by using various phase-matching types and the second step is manipulation of the generated nonlinear harmonics wave by using linear wave-shaping method. Another method of manipulating nonlinear harmonic wave is by designing the structure of nonlinear photonics crystals (NPCs), which is only one process of the generation and manipulation. The third method is by manipulating the incident fundamental frequency (FF) light in advance. The property of such incident FF light will change the property of emitted second harmonic (SH) wave. In this review, we will systematically introduce the fundamental principle and latest advances in this field and summarize the respective characteristics of these three methods.

2. The Fundamental Principle of SH Wave Generation

As we know, atoms would be polarized when the light is incident on the medium. The polarization of atoms can be express as

$$\mathbf{P} = \varepsilon_0 \chi^{(1)} \cdot \mathbf{E} + \varepsilon_0 \chi^{(2)} : \mathbf{EE} + \varepsilon_0 \chi^{(3)} \vdots \mathbf{EEE} + \cdots , \tag{1}$$

where $\chi^{(1)}$ is known as the linear susceptibility and ε_0 is the permittivity of free space. $\chi^{(2)}$ and $\chi^{(3)}$ are known as the second- and third-order nonlinear optical susceptibilities, respectively. $\mathbf{E}$ is the electric field of the incident light. According to the Maxwell equation, the wave equation can be taken to have the form

$$\nabla^2 \mathbf{E} - \mu_0 \frac{\partial^2 \mathbf{E}}{\partial t^2} = \mu_0 \frac{\partial^2 \mathbf{P}}{\partial t^2} . \tag{2}$$

Therefore, such polarization of the atoms in medium can be treated as the source of the new electromagnetic radiation. In linear optics, the polarization of the atoms only relate to the first-order of the electric field of the incident light. It can be used to explain the refraction, reflection, and transmission of the linear optical wave. In nonlinear optics, the higher order of the polarization of the atoms cannot be neglected, which causes electromagnetic radiation at new frequency. Take the SH generation as the example, the coupled wave equation can be

written as

$$\frac{dA_2}{dz} = \frac{i\omega}{cn(2\omega)} d_{\text{eff}} A_1^2 e^{-i\Delta kz},$$
$$\frac{dA_1}{dz} = \frac{i\omega}{cn(\omega)} d_{\text{eff}} A_2 A_1^* e^{i\Delta kz}, \tag{3}$$

where A_1, A_2 are, respectively, the complex amplitudes of the FF and SH waves propagating along the z-axis. d_{eff} represents the effective nonlinear coefficient, which depends on the nonlinear crystal, the direction of light wave propagation and its polarization.

$$\Delta k = k_2 - 2k_1 = k(2\omega) - 2k(\omega). \tag{4}$$

It represents the difference between wavevector of SH $k(2\omega)$ and the nonlinear polarized wave $2k(\omega)$.

In nonlinear frequency conversion process, the energy conservation determines the frequency of the generated SH wave and the momentum conservation, which also terms the phase matching relation as shown in Eq. (4), directly affects the conversion efficiency. Birefringent phase matching[15,16] and quasi-phase matching[17] are the most common phase matching methods to realize nonlinear frequency conversion, which use birefringence and structure of the nonlinear crystal to compensate the dispersion of the optical wave in different frequency, as shown in Fig. 1. In addition, not limited to these two phase matching methods, the new type of phase matching method is also a hot research topic in nonlinear fields, such as random phase matching,[18] quasi-phase matching assisted by photorefractive effect[19] or electro-optical effect,[20] and so on.[21–25]

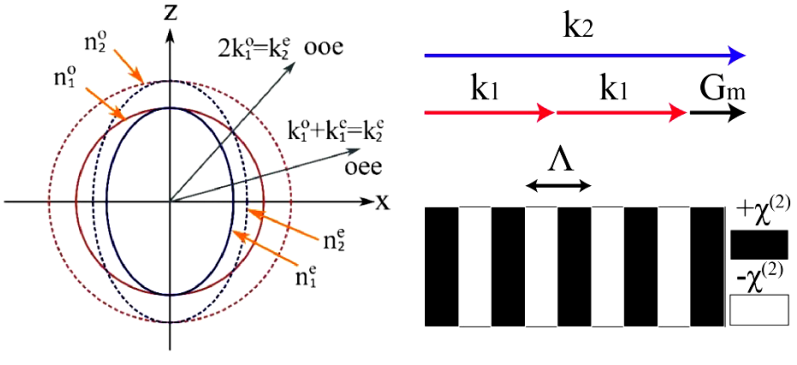

(a) (b)

Fig. 1. (a) The possible types of birefringent phase matching in negative uniaxial crystal and (b) quasi-phase matching method.

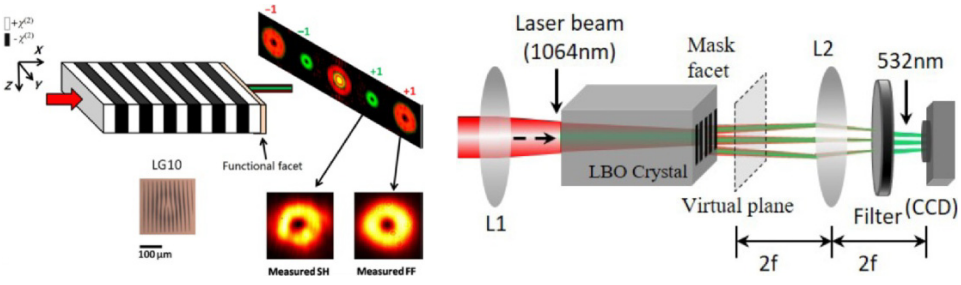

(a) (b)

Fig. 2. Two cases of the manipulation nonlinear harmonic waves using linear method.[37,39]

3. Manipulation of SH Wave by Using Linear Method

The most direct method to realize the manipulation of SH wave is by using the most mature and simple technique. Now, the linear method has been successfully used to manipulate all kinds of parameters of the optical wave, such as the phase, amplitude, polarization, angular momentum, and so on. In this process, it prompts the development of the experimental research of some special light beams like vortex beam,[26–28] vector beam,[29–31] Airy beam,[32–36] and so on. Hence, such linear method is the ideal candidate to realize the manipulation of SH wave. The whole process can be described as two steps. The first step is the generation of the SH wave by using different phase matching types and the second step is that we let the generated SH pass through the preprocessed functional facet. In recent research, FF and SH vortex can be generated at the same time when the functional facet was designed as a fork-shaped grating, as shown in Fig. 2(a).[37] Following this idea, the functional facet can also be fabricated to arbitrary shapes to generate SH waves with arbitrary phase and amplitude distribution, as shown in Fig. 2(b).[38,39]

The advantage of manipulating of SH wave by using linear method is that we can make full use of mature linear optical wave modulation methods. Its disadvantages include: (1) Due to the dispersion of optical wave in nonlinear materials, the optical elements in the original FF band cannot be directly applied to the SH waves. Hence, the modulation of SH waves is often inaccurate by using the same optical elements in FF waveband. (2) Optical elements need to be redesigned and manufactured corresponding to different wavelengths, which increases the cost and workload.

4. Manipulation of SH Wave by Using NPCs

4.1. *NPCs and its fabrication*

Since the quasi-phase matching technology was proposed, $\chi^{(2)}$ space modulation technology of the nonlinear crystals has been greatly developed in recent decades. Especially in some ferroelectric crystals, the electric field polarization technology has

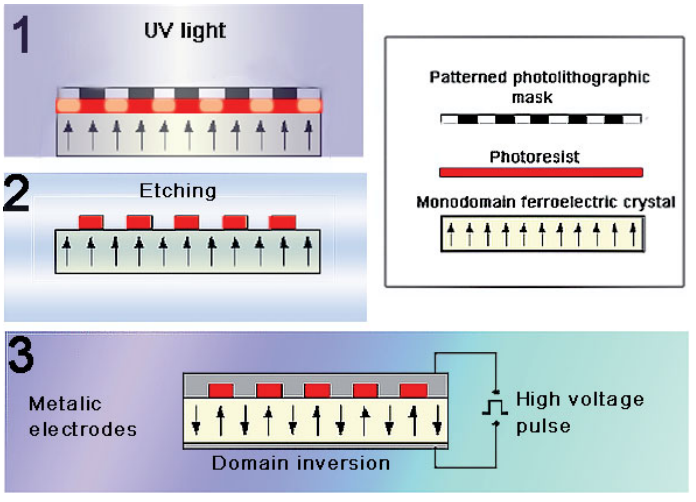

Fig. 3. The fabrication process of NPCs by using electric field poling technique.[42]

become more and more sophisticated.[40,41] By using electric field polarization technology, commercial periodically polarized ferroelectric crystals are easily available now, such as periodically polarized $LiNbO_3$, KDP, KTP (PPLN, PPKDP, PPKTP), and so on. As the correspondence of the photonic crystals in nonlinear field, researchers have also put forward the new concept of NPCs.[42] The so-called NPCs refer to the materials in which the second order susceptibility $\chi^{(2)}$ is spatially modulated while the linear susceptibility remains constant. These structures are significantly different than the more common photonic crystals, in which the linear susceptibility is modulated.

The fabrication process of NPCs by using electric field polarization technology can be briefly described as the following processes, as shown in Fig. 3[42]:

(1) The photoresist is uniformly applied to the surface of the crystal with the glue throwing machine. The prepared mask is covered on photoresist and exposed by using the ultraviolet light.
(2) After exposure by using ultraviolet light, one can remove the mask and use etchant to corrode the photoresist at the exposed or unexposed positions. In this way, the photoresist on the surface of the sample will show the same or the opposite pattern of the mask.
(3) The upper and lower surfaces of the sample are coated with metal electrodes. The high voltage pulses between electrodes of upper and lower surfaces are used to flip the domain structure of the nonlinear crystal.

In addition to electric field polarization technology, $\chi^{(2)}$ modulation of NPCs can also be realized by ion exchange,[43] electron beam radiation,[44] femtosecond laser radiation.[45–50] Electron beam radiation technology can realize domain inversion at

nanometer scale, which provides a technical path for the fabrication of nonlinear metasurface.

4.2. *Transverse modulation*

Supposing the FF light incident along the transverse direction (domain wall direction or z-axis of the NPCs), and under paraxial and small signal approximation, the coupled wave equation can be expressed as[51,52]

$$\left(\frac{\partial}{\partial z}+\frac{i}{2k_2}\frac{\partial^2}{\partial x^2}\right)A_2(x,z)=-ig(x)\beta_2 A_1^2(x)e^{i\Delta kz}, \tag{5}$$

where $A_1(x)$ and $A_2(x,z)$, respectively, represent the amplitude of FF and SH wave. $A_1(x)=A_1e^{-(x-x_0)^2/a^2}$ for the Gaussian beam. Here, A_1, x_0 and a are, respectively, the amplitude constant, the central position and the half-height width of the FF beam. $g(x)$ represents the spatial distribution function of $\chi^{(2)}$ of NPCs. $\beta_2=k_2\chi^{(2)}/(2n_2^2)$ represents the nonlinear coupling coefficient, where n_2 is the refractive index of the SH wave.

The amplitude $A_2(\kappa_x,z)$ can be expressed as the Fourier spectrum

$$A_2(\kappa_x,z)=\int A_2(x,z)e^{i\kappa_x x}dx. \tag{6}$$

Substitute it into Eq. (5)

$$\left(\frac{\partial}{\partial z}-\frac{i\kappa_x^2}{2k_2}\right)A_2(\kappa_x,z)=-i\beta_2\int g(x)A_1^2(x)e^{i\kappa_x x}e^{i\Delta kz}dx. \tag{7}$$

The amplitude of the SH in the far field can be expressed as

$$\begin{aligned}A_2(\kappa_x,z)=&-i\beta_2 z e^{iz(\Delta k+\kappa_x^2/2k_2)/2}\sin c[z(\Delta k-\kappa_x^2/2k_2)/2]\\&\times\int g(x)A_1^2(x)e^{i\kappa_x x}dx.\end{aligned} \tag{8}$$

In case of one-dimensional periodically modulated NPCs, $g(x)$ can be expanded into the form of Fourier series as:

$$g(x)=\sum_{m=0,\pm1,\pm2,\ldots}g_m e^{imG_0x}. \tag{9}$$

Here, $G_0=2\pi/\Lambda$ is the reciprocal lattice vector of the NPCs. $g_m(m\neq0)=2\sin(\pi mD)/(\pi m)$ and $g_0=2D-1$ are the Fourier coefficients. D is the duty ratio of crystal structure. Substituting Eq. (9) into Eq. (8) and considering the relationship between light intensity and amplitude of the SH $S_2(\kappa_x,z)=|A_2(\kappa_x,z)|^2$, it can be obtained that

$$\begin{aligned}S_2(\kappa_x,z)=&\pi a^2z^2\beta_2^2I_1^2\times\{\sin c[z(\Delta k-\kappa_x^2/2k_2)/2]\}^2\\&\times\left(\sum_{m=0,\pm1,\pm2,\ldots}g_m e^{-a^2(mG_0+\kappa_x)^2/8}e^{imG_0}\right)^2.\end{aligned} \tag{10}$$

From Eq. (10), three fundamental phenomena can be observed, which are nonlinear Raman-Nath diffraction, nonlinear Bragg diffraction, and nonlinear Cherenkov radiation. The last term in Eq. (10) represents the discrete Gaussian function and the corresponding SH is determined by the following relation:

$$mG_0 + \kappa_x = 0. \tag{11}$$

This expression is the nonlinear Raman-Nath diffraction condition: $\kappa_x = -mG_0 = k_2 \sin\alpha_m$.

According to Eq. (10), $\Delta k - \kappa_x^2/2k_2 = 0$ when $\sin c[z(\Delta k - \kappa_x^2/2k_2)/2]$ reaches its maximum. $k_2^2 = \kappa_x^2 + (2k_1)^2$ when the condition $[1 - (\kappa_x/k_2)]^{1/2} \approx 1 - \kappa_x/2k_2$ is satisfied. Then, the nonlinear Cherenkov condition can be obtained as follows:

$$k_2 \cos\theta_C = 2k_1. \tag{12}$$

Nonlinear Bragg diffraction depends on both Eqs. (11) and (12). Namely, nonlinear Bragg diffraction can be treated as the resonance condition of the nonlinear Raman-Nath diffraction and nonlinear Cherenkov radiation.[53–55] The schematic diagrams and the phase-matching conditions of these three fundamental phenomena can be shown in Fig. 4.

According to Eq. (10), the pattern of nonlinear Raman-Nath SH in the far field is proportional to the Fourier transform of $\chi^{(2)}$ structure in NPCs. In fact, such Fourier transform relation between the structure of the NPCs and the SH in the far field also keep in two-dimensional case. Therefore, the SH can be manipulated by changing $\chi^{(2)}$ structure of NPCs. For example, the $\chi^{(2)}$ structure of NPCs can be modulated as

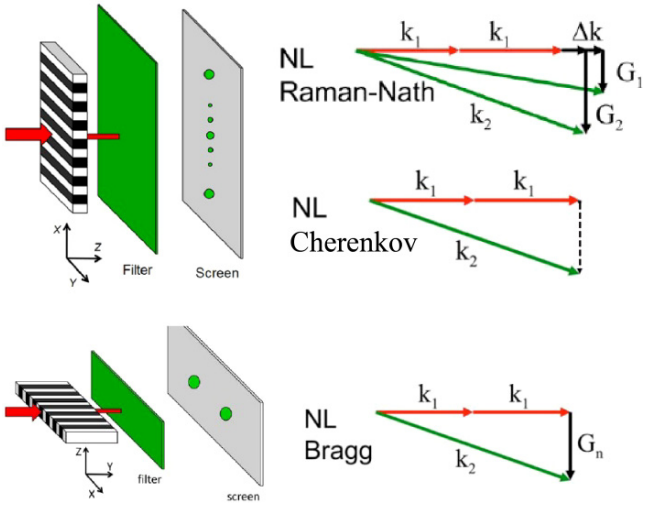

Fig. 4. Schematic diagrams and the phase-matching conditions of the nonlinear Raman-Nath diffraction, nonlinear Cherenkov radiation, and nonlinear Bragg diffraction.[53–55]

the following form[56]:

$$\chi^{(2)}(x,y) = d_{ij}\mathrm{Sign}\{\cos[2\pi f_{\mathrm{carrier}}x - \phi(x,y)] - \cos[\pi q(x,y)]\}, \tag{13}$$

where f_{carrier} represents the spatial frequency of the nonlinear grating. $\phi(x,y)$ and $q(x,y)$ represent the modulation parameters of the nonlinear grating. The Fourier transform corresponding to this nonlinear grating can be written as

$$F[\chi^{(2)}(x,y)] = \sum_{m=-\infty}^{\infty}\left\{\frac{\sin[m\pi q(x,y)]}{m\pi} \times \exp[im(2\pi f_{\mathrm{carrier}}x + \phi(x,y))]\right\}. \tag{14}$$

Therefore, the +1-order of nonlinear Raman-Nath diffraction can be written as

$$E(2\omega) \propto \sin[\pi q(x,y)]\exp[i\phi(x,y)]. \tag{15}$$

The amplitude and phase of the generated SH are completely determined by the structure parameters of the NPCs. Following this principle, the SH vortex beam $E(2\omega) \propto F[\chi^{(2)}(x,y)] \propto \exp(iml_c\phi)$ can be generated when the structure of NPCs modulated as the fork-shaped grating $\chi^{(2)}(x,y) = d_{ij}\mathrm{Sign}\{\cos[2\pi f_{\mathrm{carrier}}x - l_c\phi]\}$, as shown in Fig. 5(a).[57] Here, l_c represents the topological charge of the NPCs. In addition, SH Hermitian Gaussian (HG) beam and SH Laguerre Gaussian (LG) beam can also be realized by using the same method,[56] as shown in Fig. 5(b). Theoretically, SH with arbitrary amplitude and phase can be generated by using this method.

However, we can see that the nonlinear Raman-Nath diffraction process is a phase-mismatching process, as shown in Fig. 4. Therefore, the conversion efficiency of the SH generation process is quite low. To further improve the conversion efficiency of nonlinear Raman-Nath diffraction, nonlinear Bragg diffraction can be used to solve this problem to some extent. Figure 6 shows the manipulating SH by using nonlinear Bragg diffraction. In this case, the NPCs are tilted to satisfy the nonlinear Bragg condition.[58]

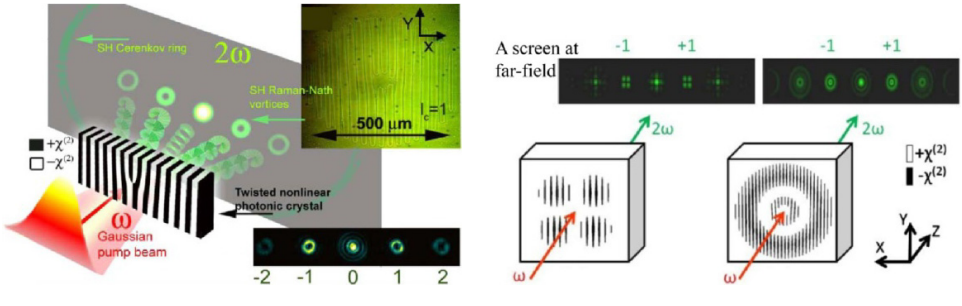

Fig. 5. (a) The generation of second-order harmonic nonlinear vortices by using a twisted NPC[57] and (b) the generation of HG_{11} and LG_{11} in the first-order of nonlinear Raman-Nath spot by utilizing the two-dimensional (2D) modulated NPCs.[56]

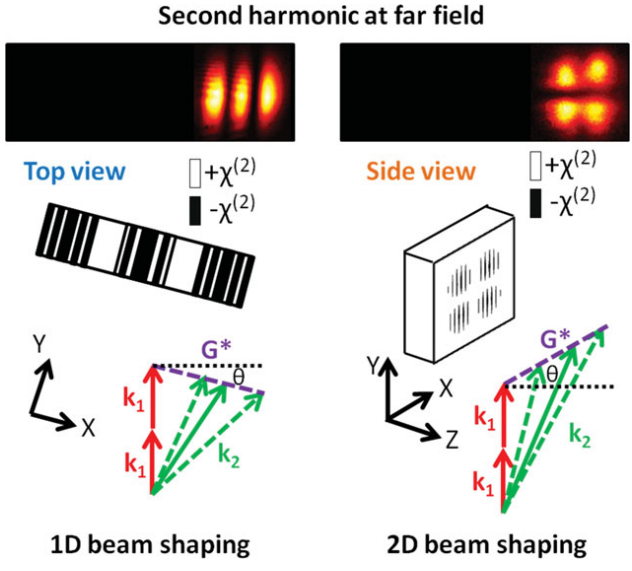

Fig. 6. 1D (HG_{20}) and 2D (LG_{11}) SH manipulating by using nonlinear Bragg diffraction.[58]

4.3. *Longitudinal modulation*

In the case of longitudinal modulation process, the incident FF beam propagates along the quasi-phase matching direction. Assuming that the FF beam propagates along z-axis (here, z-axis only represents the propagation direction and independents to the optical axis of the crystal), the coupled wave equation can be rewritten as the following expression under the paraxial and small signal approximation[42,59]:

$$\frac{dA_2(z)}{dz} = \frac{i\omega}{cn(2\omega)} A_1^2 d_{\text{eff}}(z)\exp[-i(k_2 - 2k_1)z], \tag{16}$$

where $d_{\text{eff}}(z) = d_{\text{eff}} \cdot g(z)$ represents the modulation of the nonlinear coefficient along the light propagation direction, which can be written as the product of the effective nonlinear coefficient d_{eff} and the spatial modulation function $g(z)$ of the nonlinear coefficient. When the FF light passes through a nonlinear crystal with the length of L, the amplitude of the SH can be expressed as

$$A_2(L) = \frac{i\omega}{cn(2\omega)} d_{\text{eff}} A_1^2 \int_{-\infty}^{\infty} g(z)\exp(-i\Delta kz)dz. \tag{17}$$

It can be seen that the SH emitted from the exit facet of the crystal is proportional to the Fourier transform of $g(z)$, which can be expressed as

$$G(\Delta k) = \frac{1}{L} \int_{-\infty}^{\infty} g(z)\exp(-i\Delta kz)dz. \tag{18}$$

Therefore, the amplitude of the generated SH can be represented as

$$A_2(L) = \frac{i\omega}{cn(2\omega)} d_{\text{eff}} L A_1^2 G(\Delta k). \tag{19}$$

Therefore, both the amplitude and phase of the SH can be manipulated by designing the structure parameters of the NPCs. For example, the structure of the NPC can be modulated into the following form[60]:

$$\chi^{(2)}(x, y) = d_{ij}\text{Sign}\{\cos[2\pi f_x x - \phi(y)] - \cos[\pi q(y)]\}. \tag{20}$$

Only considering the case of +1-order reciprocal lattice vector of the NPCs to fulfil the phase matching condition, the generated SH can be expressed as

$$E(2\omega) \propto \sin[\pi q(y)]\exp[i\phi(y)]. \tag{21}$$

Similar to the case of transverse modulation, the amplitude and phase of the generated SH are completely determined by the structure parameters of the NPCs. Following this principle, the generated SH on the exit facet of the crystal is proportional to the phase distribution of the Airy beam $\exp(if_c y^3)$ when the structure of NPCs modulated as the following form $\chi^{(2)}(x, y) = d_{ij}\text{Sign}[\cos(2\pi f_x x + f_c y^3)]$, as shown in Fig. 7(a).[61] Here, f_x and $f_{c'}$ respectively, represents the spatial frequency along the propagation direction and the modulation intensity along the transverse direction of the FF beam. In this case, the phase matching relation can be expressed as: $2\pi f_x = k_2 - 2k_1$. In addition, 1D SH HG (HG_{01} and HG_{03}) beam and 1D SOS Morse-coded function: three Gaussians (for the three short pulses of "S" in Morse code), three super-Gaussians (for the three long pulses of the "O" in Morse code) beam can also be realized in the near-field by using this method, as shown in Fig. 7(b).[60] Theoretically, 1D SH with arbitrary amplitude and phase can be generated by using this method.

Furthermore, some important theories were also proposed for designing the structure of NPCs to realize arbitrary SH manipulation. For example, nonlinear Huygens–Fresnel principle[62] is proposed to realize the SH manipulation based on the local phase matching in nonlinear frequency conversion, as shown in Fig. 8(a). The

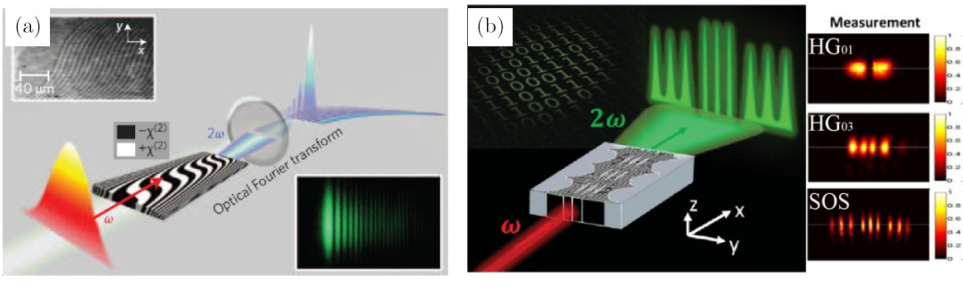

Fig. 7. (a) The generation of nonlinear Airy beam[61] and (b) schematic of on-axis 1D near-field SH shaping by using NPCs.[60]

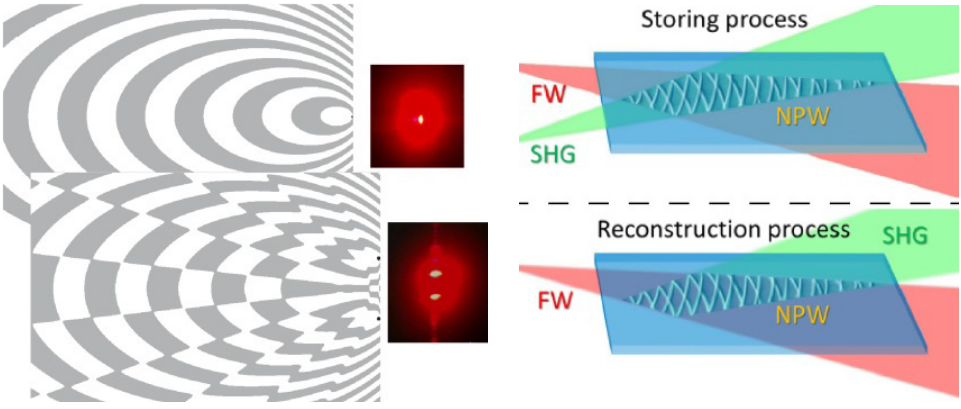

Fig. 8. (a) Nonlinear Huygens-Fresnel principle[62] and (b) nonlinear volume holography.[63]

concept of the nonlinear volume holography[63] is also an important theoretical extension to the well-know volume holography concept in the linear optical field, as shown in Fig. 8(b).

Manipulation of SH wave by using the structure of the NPCs has advantages in the field of integrated photonics because of its compact structure. However, this method also has its own disadvantages: First, domain inversion can only be carried out in a fixed direction due to the intrinsic atomic arrangement of crystals. For example, domain inversion is only along z-axis in $LiNbO_3$, $LiTaO_3$ crystals. Therefore, only 1D modulation of the SH wave can be realized along the longitudinal direction of the crystal. In order to realize 2D modulation of the SH wave, FF light needs to be incident along the transverse direction. For nonlinear Raman-Nath diffraction, the efficiency of the SH generation is quite low due to the phase mismatch in the propagation direction. Nonlinear Bragg diffraction can increase the conversion efficiency of the SH in some extent, but the modulated SH can only be generated on one side. Secondly, the original value of $\chi^{(2)}$ becomes negative after domain inversion process. Therefore, different domains of NPCs only produce 0 or π modulation for the SH waves. Finally, once the crystal structure is fabricated, it is difficult to change its structural characteristics. Therefore, the SH generated by using this method cannot be dynamically changed.

4.4. *Three dimension NPCs*

Since the first proposition of three-dimensional (3D) NPCs in theory,[64,65] two research groups independent realize three-dimensional NPCs in the experiment by using femtosecond laser direct writing technology in recent years,[66,67] which offer a new degree of freedom to manipulate the SH waves. In this structure, the reciprocal

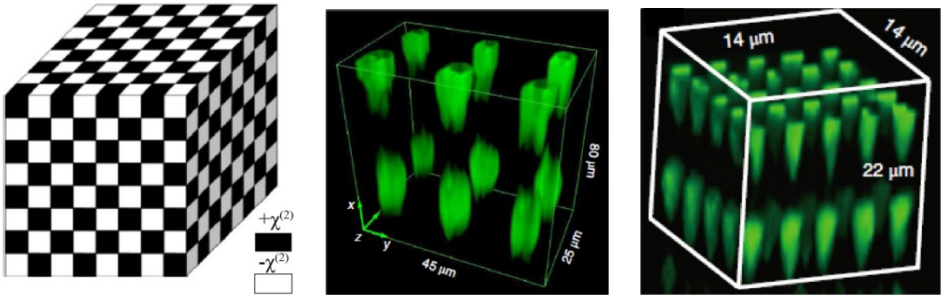

(a) (b) (c)

Fig. 9. (a) Show the schematic of the structure of 3D NPCs,[64] (b) and (c) show the structure of 3D NPCs realized in the experiment.[66,67]

lattice vectors of the crystal $\mathbf{G}_{m,n,l}$ exist in 3D direction

$$\mathbf{G}_{m,n,l} = \frac{2\pi m}{\Lambda_x}\mathbf{x} + \frac{2\pi n}{\Lambda_y}\mathbf{y} + \frac{2\pi l}{\Lambda_z}\mathbf{z}. \tag{22}$$

Here, Λ_x, Λ_y and Λ_z are, respectively, the period of the 3D NPCs along x, y and z direction. Figure 9(a) show the schematic of the structure of 3D NPCs. Figures 9(b) and 9(c) show the structure of 3D NPCs realized in the experiment in recent works.

By using such 3D NPCs, most of the disadvantages of manipulating SH by using structure of the NPCs summarized above could be overcome. For example, it can realize phase matching in arbitrary direction to increase the conversion efficiency of the generated SH. By using 3D structure, not only 1D and 2D manipulation of the generated SH, but also 3D shaping of the SH with high conversion efficiency can be realized. Unfortunately, the femtosecond laser direct writing technology is still not mature enough to realize 3D $\chi^{(2)}$ modulation because only a few layers can be fabricated in the propagation direction of the femtosecond laser. Therefore, it still has a long way to go.

5. Manipulation of the SH Wave by Using Structured FF Light

In addition to the method mentioned before, the manipulation of SH can also be realized by modulating the structure of FF light in advance,[68] as shown in Fig. 10. By using slow-varying amplitude approximation, the couple wave equation satisfies the following relation when the FF light propagates along the z-axis:

$$\nabla_T^2 A_{2\omega} + 2ik_2 \frac{\partial A_{2\omega}}{\partial z} = -\kappa A_\omega^2 e^{i(2k_1 - k_2)z}, \tag{23}$$

where A_ω and $A_{2\omega}$ denote the complex amplitude of FF light and SH, respectively. $\nabla_T^2 = \partial^2/\partial x^2 + \partial^2/\partial y^2$ represents the 2D Laplace operator of the transverse direction. $\kappa = \chi^{(2)}\omega_2^2/c^2$ represents the nonlinear coupling coefficient. In case of phase matching condition $2k_1 - k_2 = 0$, $\exp[i(2k_1 - k_2)z] = 1$. The diffraction effect of FF

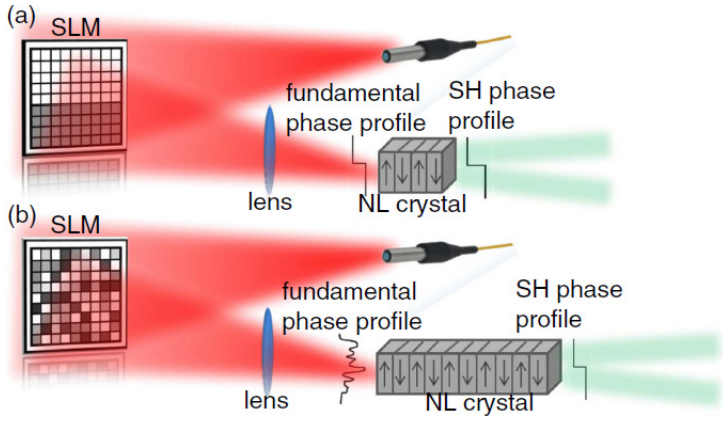

Fig. 10. Realizing SH shaping by modulating FF beam.[68]

light can be ignored if the nonlinear crystal is short enough. In this way, the couple wave equation can be rewritten as

$$\frac{dA_{2\omega}}{dz} = -\frac{i\kappa}{2k_2}A_{\omega}^{2}. \tag{24}$$

The complex amplitude of the incident FF light can be written as $A_{\omega} = |A_{\omega}|\exp(i\varphi_{\omega})$. Under small signal approximation, the SH can be obtained

$$A_{2\omega}(x,y) \approx -\frac{i\kappa}{2k_2}|A_{\omega}(x,y)|^{2}e^{i2\varphi_{\omega}(x,y)}L. \tag{25}$$

We can see that the amplitude and phase of the generated SH can be manipulated by the amplitude and phase of the incident FF beam. Following this method, SH beams such as different types of HG beam and Airy beam[68,69] have been achieved, as shown in Fig. 11.

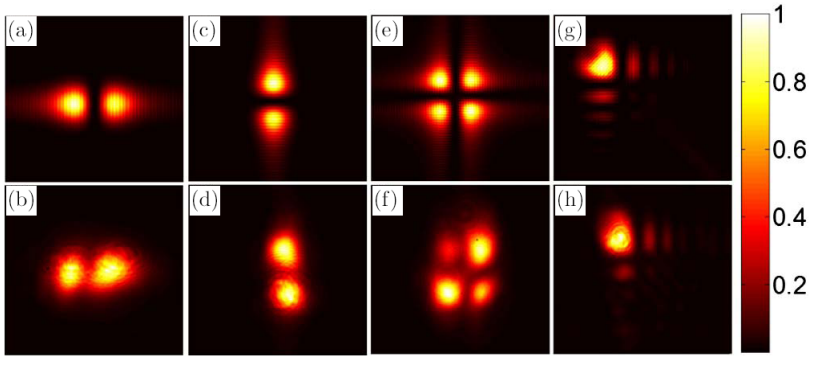

Fig. 11. Simulated (top) and experimental (bottom) results of generating the following SH beams: (a) and (b) HG_{01}, (c) and (d) HG_{10}, (e) and (f) HG_{11}, (g) and (h) 2D Airy beam.[68]

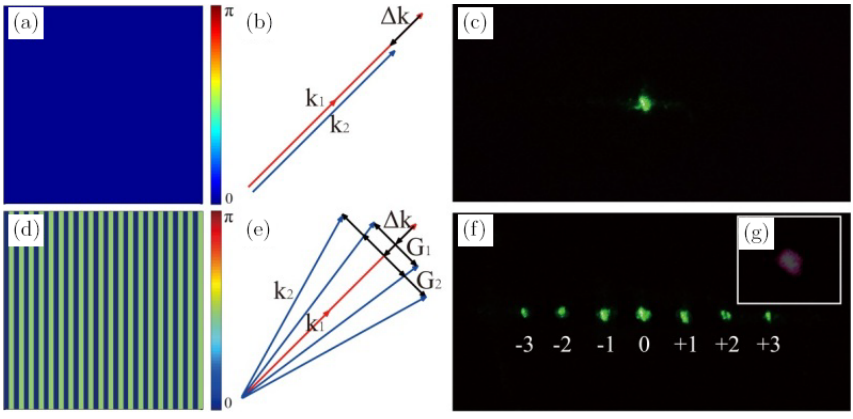

Fig. 12. (a)(d) The phase structure of the FW, (b)(e) the corresponding phase-matching geometries of the nonlinear Raman-Nath SH, (c)(f) observed SH diffraction patterns in the far field and (g) the profile of the FW at end of the nonlinear crystal.[70]

The concept of structured FF beam, of which the phase in the cross-section of the beam was modulated as some special structures, was introduced to the nonlinear frequency conversion process in our recent works.[70–76] The diffraction of SH originates from the structure modulation of the phase of the FF beam, rather than the grating of an NPC. In our work, we bring more attention to the concept of spatial structure of the FF beam, which not only mimics the effects as those in NPCs but also exhibits much more flexibility and controllability in manipulating SH waves.

It has been demonstrated that nonlinear Raman-Nath SH can be dynamically achieved when the phase periodically modulated FF beam is incident on a homogeneous nonlinear crystal,[70] as shown in Fig. 12. The first row shows the case of FF beam without phase modulating. The second row shows nonlinear Raman-Nath SH generation when the phase of FF beam is periodically modulated. It is different with the SH diffraction effect observed in NPCs. In NPCs, the SH diffraction originates from the structure of the nonlinear grating. In our method, the diffraction of Raman-Nath SH comes from the phase changes of the structured FF beam. Besides, nonlinear Raman-Nath SH generation of hybrid structured FW, which combine periodic and random structure of the FF phase, was also investigated.[71] In this case, more diffraction spots can be obtained and the intensity and directions of generated SH can be manipulated by the phase structure of the FF beam.

Nonlinear vortex beam array can also be generated by utilizing an FF beam with fork-shaped phase structure incident on a homogeneous nonlinear crystal.[72] The topological charge of SH vortex beam of different diffraction orders located in such SH vortex beam array can be measured by a cylindrical lens. Figures 13(a) and 13(b), respectively, show 1D and 2D nonlinear vortex beam array generation when the phase of the FF beam was modulated as 1D and 2D fork-shaped grating structure.

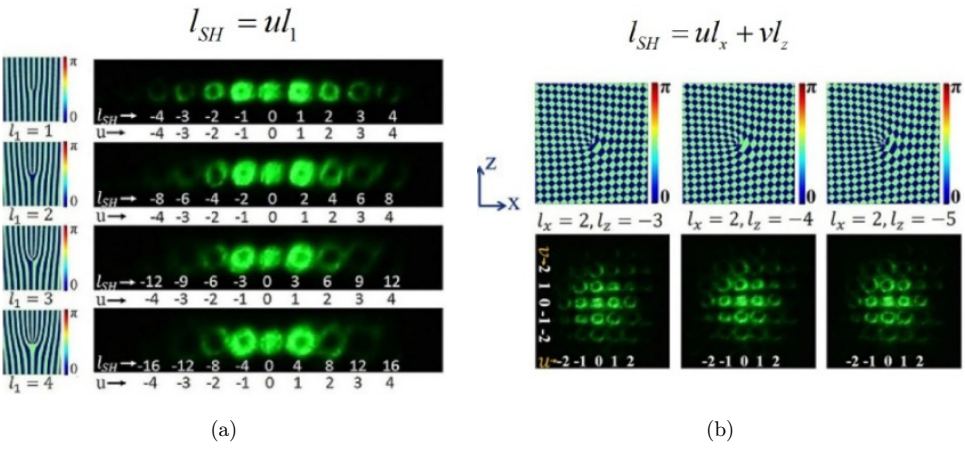

Fig. 13. (a) 1D and (b) 2D nonlinear vortex beam arrays generation when different phase structures of the FW incident into the nonlinear bulk crystal.[72]

In 1D case, the topological charge of SH in different orders obeys the law $l_{\mathrm{SH}} = ul_1$. In 2D case, the topological charge of SH in different orders obeys the law $l_{\mathrm{SH}} = ul_x + vl_z$. In addition to pure phase modulation of the SH, we can also realize the modulation of amplitude and phase in the +1-order diffraction of the SH. In our recent works, amplitude modulated LG SH beams (including LG_{10} and LG_{20}) and LG_{11} SH beam with the both modulated amplitude and phase were generated.[73]

Nonlinear holography technique is a powerful tool for all optical switching and manipulation of arbitrary nonlinear harmonic waves. In previous works, the method of realizing such nonlinear holography is by configuring the structure of NPCs.[63,77] However, it is a challenge to dynamically tune the nonlinear harmonic wave pattern. To overcome the long-term existed non-dynamic property of such nonlinear holographs, the method of the combination of dynamic computer-generated optical holograms and noncollinear SH generation process is proposed in our recent work.[74] In our experiment, arbitrary patterns both in FF and SH waveband can be generated at the same time. Compared with previous works, this method does not need complex arrangement of optical components and fabrication of the NPCs. Figures 14(a) and 14(b) show the schematic of the experimental setup and the phase-matching diagram, respectively. To illustrate the dynamic property of our method, a running horse is experimentally realized, as shown in Fig. 14(c).

In addition to the amplitude and phase modulation of the SH, we also realized the polarization manipulating of the SH in our recent work,[78] as shown in Fig. 15. It is a challenge to realize nonlinear frequency conversion and manipulation of vector beams because of the polarization sensitivity in most of the nonlinear processes. In our experiment, we generate SH vector beams by using three-wave mixing processes, which occur in two orthogonal placed nonlinear crystals, and the vector property is recognized by using a Glan–Taylor polarizer. FF vector beam can be written as

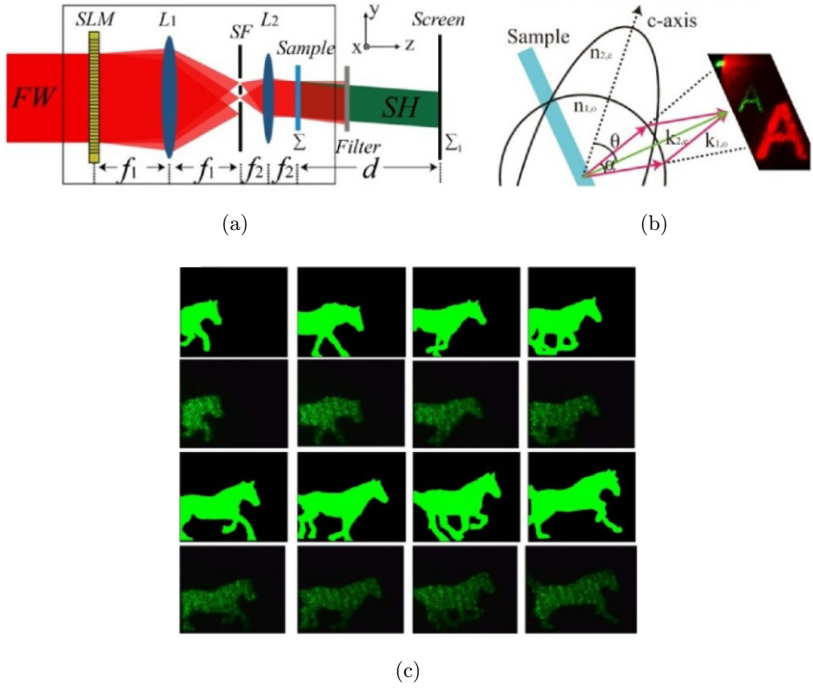

Fig. 14. (a) Schematic of the experimental setup to realize dynamic nonlinear holography. SLM: spatial light modulator; SF: spatial filter; Sample: 5 mol.% MgO:$LiNbO_3$, (b) phase-matching diagram of the noncollinear SHG process and (c) a running horse is realized in the experiment.[74]

$E(\omega) = [\cos(m\varphi + \varphi_0), \sin(m\varphi + \varphi_0)]$. Here, φ, m and φ_0 are the azimuth angle, topological charge, and the initial phase of the vector beams, respectively. When such vector beams pass through two orthogonal placed nonlinear crystals, oo-e birefringent phase matching process is used in our experiment, the generated SH vector

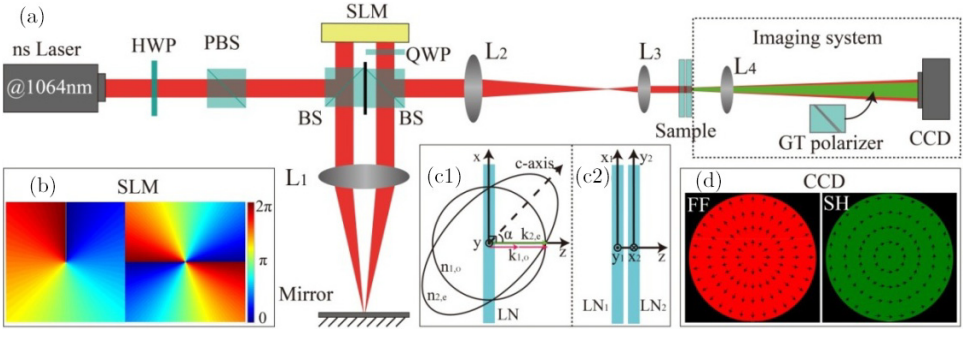

Fig. 15. (a) Schematic of the experimental setup. Sample: two orthogonal placed quadratic nonlinear crystals, (b) the phase loaded on SLM, (c1) and (c2) are, respectively, phase matching type and relative position of two $LiNbO_3$ crystals (LN1 and LN2) and (d) the polarization and intensity distribution of radially polarized FF vector beam and the corresponding generated SH vector beam.[78]

beam can be expressed as

$$E(2\omega) = \frac{i\omega d_{\text{eff}} L}{cn(2\omega)} \cdot \begin{pmatrix} \sin^2(m\varphi + \varphi_0) \\ \cos^2(m\varphi + \varphi_0) \end{pmatrix}. \tag{26}$$

It can be seen that the generated SH waves still keep the vector property. Therefore, we can realize the polarization manipulation of the SH by using this method.

The advantages of the method of modulating the SH through the FF light are as follows: (1) It can make full use of the mature technology of linear light wave modulation, especially the modulation of the FF light through the spatial light modulator. It is a flexible way to realize dynamical modulation of the nonlinear harmonic. (2) The phase of the FF light can be almost continuously changed. Therefore, the phase of the generated SH can also be continuously changed by using this method. (3) The modulation element of FF waveband can be fully utilized without redesigning the optical element corresponding to the SH. However, the disadvantage of this method is that the amplitude and the phase of the generated SH are sensitive to the nonlinear crystal length. It means that the shorter the length of the nonlinear crystal, the more accurate the parameters of the generated SH. In case of the longer crystal, there is no analytical solution of the generated SH, which requires the assistance of optimization algorithm to accurately manipulate the SH parameters.

6. Conclusion

In this review, we have systematically introduced the fundamental principle and latest advances of SH waves manipulation. Intuitively, there are three methods to manipulate such SH waves according to the sequence of generation and manipulation, which are tailoring the functional facet, the structure of crystals, and the structure of the incident FF light. At the end of each method, we also systematically summarize their respective advantages and disadvantages.

Acknowledgments

The authors thank the National Key R&D Program of China (2018YFA0306301, 2017YFA0303701); National Natural Science Foundation of China (NSFC) (11734011); and the Foundation for Development of Science and Technology of Shanghai (17JC1400400).

References

1. J. Ng, Z. Lin and C. T. Chan, Theory of optical trapping by an optical vortex beam, *Phys. Rev. Lett.* **104**(10) (2010) 103601.
2. K. T. Gahagan and G. A. Swartzlander, Simultaneous trapping of low-index and high-index microparticles observed with an optical-vortex trap, *J. Opt. Soc. Am. B* **16**(4) (1999) 533–537.

3. S. H. Tao, X. C. Yuan, J. Lin *et al.*, Fractional optical vortex beam induced rotation of particles, *Opt. Exp.* **13**(20) (2005) 7726–7731.
4. M. Meier, V. Romano and T. Feurer, Material processing with pulsed radially and azimuthally polarized laser radiation, *Appl. Phys. A* **86**(3) (2007) 329–334.
5. J. Chu, X. Li, Q. Smithwick *et al.*, Coding/decoding two-dimensional images with orbital angular momentum of light, *Opt. Lett.* **41**(7) (2016) 1490–1493.
6. M. K. Sharma, J. Joseph and P. Senthilkumaran, Selective edge enhancement using anisotropic vortex filter, *Appl. Opt.* **50**(27) (2011) 5279–5286.
7. A. Vaziri, J. W. Pan, T. Jennewein *et al.*, Concentration of higher dimensional entanglement: Qutrits of photon orbital angular momentum, *Phys. Rev. Lett.* **91**(22) (2003) 227902.
8. J. Leach, B. Jack, J. Romero *et al.*, Violation of a Bell inequality in two-dimensional orbital angular momentum state-spaces, *Opt. Exp.* **17**(10) (2009) 8287–8293.
9. R. Fickler, R. Lapkiewicz, W. N. Plick *et al.*, Quantum entanglement of high angular momenta, *Science* **338**(6107) (2012) 640–643.
10. M. Malik, M. Erhard, M. Huber *et al.*, Multi-photon entanglement in high dimensions, *Nature Photonic.* **10**(4) (2016) 248.
11. J. Wang, J. Y. Yang, I. M. Fazal *et al.*, Terabit free-space data transmission employing orbital angular momentum multiplexing, *Nature Photonic.* **6**(7) (2012) 488.
12. G. Milione, M. P. J. Lavery, H. Huang *et al.*, 4×20 Gbit/s mode division multiplexing over free space using vector modes and a q-plate mode (de) multiplexer, *Opt. Lett.* **40**(9) (2015) 1980–1983.
13. Y. Zhao and J. Wang, High-base vector beam encoding/decoding for visible-light communications, *Opt. Lett.* **40**(21) (2015) 4843–4846.
14. W. Han, Y. Yang, W. Cheng *et al.*, Vectorial optical field generator for the creation of arbitrarily complex fields, *Opt. Exp.* **21**(18) (2013) 20692–20706.
15. A. Rose and D. R. Smith, Overcoming phase mismatch in nonlinear metamaterials, *Opt. Mater. Exp.* **1**(7) (2011) 1232–1243.
16. A. Fiore, S. Janz, L. Delobel *et al.*, Second-harmonic generation at $\lambda = 1.6\,\mu$m in AlGaAs/Al2O3 waveguides using birefringence phase matching, *Appl. Phys. Lett.* **72**(23) (1998) 2942–2944.
17. J. A. Armstrong, N. Bloembergen, J. Ducuing *et al.*, Interactions between light waves in a nonlinear dielectric, *Phys. Rev.* **127**(6) (1962) 1918.
18. M. Baudrier-Raybaut, R. Haidar, P. Kupecek *et al.*, Random quasi-phase-matching in bulk polycrystalline isotropic nonlinear materials, *Nature* **432**(7015) (2004) 374.
19. A. S. Kewitsch, M. Segev, A. Yariv *et al.*, Tunable quasi-phase matching using dynamic ferroelectric domain gratings induced by photorefractive space-charge fields, *Appl. Phys. Lett.* **64**(23) (1994) 3068–3070.
20. Z. Cui, D. Liu, J. Miao *et al.*, Phase matching using the linear electro-optic effect, *Phys. Rev. Lett.* **118**(4) (2017) 043901.
21. Z. D. Xie, X. J. Lv, Y. H. Liu *et al.*, Cavity phase matching via an optical parametric oscillator consisting of a dielectric nonlinear crystal sheet, *Phys. Rev. Lett.* **106**(8) (2011) 083901.
22. A. Rose, D. Huang and D. R. Smith, Controlling the second harmonic in a phase-matched negative-index metamaterial, *Phys. Rev. Lett.* **107**(6) (2011) 063902.
23. M. Kauranen, Freeing nonlinear optics from phase matching, *Science* **342**(6163) (2013) 1182–1183.
24. P. S. Kuo, J. Bravo-Abad and G. S. Solomon, Second-harmonic generation using quasi-phase matching in a GaAs whispering-gallery-mode microcavity, *Nature Comm.* **5** (2014) 3109.

25. I. Breunig, Three-wave mixing in whispering gallery resonators, *Laser Photonic. Rev.* **10** (4) (2016) 569–587.
26. L. Allen, M. W. Beijersbergen, R. J. C. Spreeuw *et al.*, Orbital angular momentum of light and the transformation of Laguerre-Gaussian laser modes, *Phys. Rev. A* **45**(11) (1992) 8185.
27. A. M. Yao and M. J. Padgett, Orbital angular momentum: Origins, behavior and applications, *Adv. Opt. Photonic.* **3**(2) (2011) 161–204.
28. M. Mirhosseini, O. S. Magana-Loaiza, C. Chen *et al.*, Rapid generation of light beams carrying orbital angular momentum, *Opt. Exp.* **21**(25) (2013) 30196–30203.
29. H. Chen, J. Hao, B. F. Zhang *et al.*, Generation of vector beam with space-variant distribution of both polarization and phase, *Opt. Lett.* **36**(16) (2011) 3179–3181.
30. X. L. Wang, J. Ding, W. J. Ni *et al.*, Generation of arbitrary vector beams with a spatial light modulator and a common path interferometric arrangement, *Opt. Lett.* **32**(24) (2007) 3549–3551.
31. S. Chen, X. Zhou, Y. Liu *et al.*, Generation of arbitrary cylindrical vector beams on the higher order Poincaré sphere, *Opt. Lett.* **39**(18) (2014) 5274–5276.
32. G. A. Siviloglou, J. Broky, A. Dogariu *et al.*, Observation of accelerating Airy beams, *Phys. Rev. Lett.* **99**(21) (2007) 213901.
33. G. A. Siviloglou and D. N. Christodoulides, Accelerating finite energy Airy beams, *Opt. Lett.* **32**(8) (2007) 979–981.
34. J. Broky, G. A. Siviloglou, A. Dogariu *et al.*, Self-healing properties of optical Airy beams, *Opt. Exp.* **16**(17) (2008) 12880–12891.
35. P. Polynkin, M. Kolesik, J. V. Moloney *et al.*, Curved plasma channel generation using ultraintense Airy beams, *Science* **324**(5924) (2009) 229–232.
36. G. A. Siviloglou, J. Broky, A. Dogariu *et al.*, Ballistic dynamics of Airy beams, *Opt. Lett.* **33**(3) (2008) 207–209.
37. A. Shapira, A. Libster, Y. Lilach *et al.*, Functional facets for nonlinear crystals, *Opt. Comm.* **300** (2013) 244–248.
38. S. Lightman, R. Gvishi, G. Hurvitz *et al.*, Shaping of light beams by 3D direct laser writing on facets of nonlinear crystals, *Opt. Lett.* **40**(19) (2015) 4460–4463.
39. D. Singh, R. Shiloh and A. Arie, Shaping the fundamental and second harmonic beams using patterned facets in lithium triborate, *Opt. Mater. Exp.* **8**(9) (2018) 2654.
40. M. Yamada, N. Nada, M. Saitoh *et al.*, First-order quasi-phase matched LiNbO3 waveguide periodically poled by applying an external field for efficient blue second-harmonic generation, *Appl. Phys. Lett.* **62**(5) (1993) 435–436.
41. S. Moscovich, A. Arie, R. Urneski *et al.*, Noncollinear second-harmonic generation in submicrometer-poled RbTiOPO4, *Opt. Exp.* **12**(10) (2004) 2236–2242.
42. A. Arie and N. Voloch, Periodic, quasi-periodic, and random quadratic nonlinear photonic crystals, *Laser Photonic. Rev.* **4**(3) (2010) 355–373.
43. M. M. Fejer, G. A. Magel, D. H. Jundt *et al.*, Quasi-phase-matched second harmonic generation: Tuning and tolerances, *IEEE J. Quantum Electronic.* **28**(11) (1992) 2631–2654.
44. M. Houe and P. D. Townsend, An introduction to methods of periodic poling for second-harmonic generation, *J. Phys. D: Appl. Phys.* **28**(9) (1995) 1747.
45. S. Fahy and R. Merlin, Reversal of ferroelectric domains by ultrashort optical pulses, *Phys. Rev. Lett.* **73**(8) (1994) 1122.
46. H. Zhu, X. Chen, H. Chen *et al.*, Formation of domain reversal by direct irradiation with femtosecond laser in lithium niobate, *Chin. Opt. Lett.* **7**(2) (2009) 169–172.
47. H. Lao, H. Zhu and X. Chen, Threshold fluence for domain reversal directly induced by femtosecond laser in lithium niobate, *Appl. Phys. A* **101**(2) (2010) 313–317.

48. X. Chen, P. Karpinski, V. Shvedov *et al.*, Ferroelectric domain engineering by focused infrared femtosecond pulses, *Appl. Phys. Lett.* **107**(14) (2015) 141102.
49. S. Kroesen, K. Tekce, J. Imbrock *et al.*, Monolithic fabrication of quasi phase-matched waveguides by femtosecond laser structuring the χ (2) nonlinearity, *Appl. Phys. Lett.* **107**(10) (2015) 101109.
50. X. Chen, P. Karpinski, V. Shvedov *et al.*, Quasi-phase matching via femtosecond laser-induced domain inversion in lithium niobate waveguides, *Opt. Lett.* **41**(11) (2016) 2410–2413.
51. Y. Sheng, Q. Kong, W. Wang *et al.*, Theoretical investigations of nonlinear Raman–Nath diffraction in the frequency doubling process, *J. Phys. B: Atomic, Molecular Opt. Phys.* **45**(5) (2012) 055401.
52. Y. Sheng, Q. Kong, V. Roppo *et al.*, Theoretical study of Čerenkov-type second-harmonic generation in periodically poled ferroelectric crystals, *J. Opt. Soc. Am. B* **29**(3) (2012) 312–318.
53. S. M. Saltiel, D. N. Neshev, W. Krolikowski *et al.*, Multiorder nonlinear diffraction in frequency doubling processes, *Opt. Lett.* **34**(6) (2009) 848–850.
54. K. Kalinowski, P. Roedig, Y. Sheng *et al.*, Enhanced Čerenkov second-harmonic emission in nonlinear photonic structures, *Opt. Lett.* **37**(11) (2012) 1832–1834.
55. A. Shapira and A. Arie, Phase-matched nonlinear diffraction, *Opt. Lett.* **36**(10) (2011) 1933–1935.
56. A. Shapira, R. Shiloh, I Juwiler *et al.*, Two-dimensional nonlinear beam shaping, *Opt. Lett.* **37**(11) (2012) 2136–2138.
57. N. V. Bloch, K. Shemer, A. Shapira *et al.*, Twisting light by nonlinear photonic crystals, *Phys. Rev. Lett.* **108**(23) (2012) 233902.
58. A. Shapira, I. Juwiler and A. Arie, Tunable nonlinear beam shaping by non-collinear interactions, *Laser Photonic. Rev.* **7**(4) (2013) L25–L29.
59. A. Shapira, L. Naor and A. Arie, Nonlinear optical holograms for spatial and spectral shaping of light waves, *Sci. Bull.* **60**(16) (2015) 1403–1415.
60. S. Trajtenberg-Mills, I. Juwiler and A. Arie, On-axis shaping of second-harmonic beams, *Laser Photonic. Rev.* **9**(6) (2015) L40–L44.
61. T. Ellenbogen, N. Voloch-Bloch, A. Ganany-Padowicz *et al.*, Nonlinear generation and manipulation of Airy beams, *Nature Photonic.* **3**(7) (2009) 395.
62. Y. Qin, C. Zhang, Y. Zhu *et al.*, Wave-front engineering by Huygens-Fresnel principle for nonlinear optical interactions in domain engineered structures, *Phys. Rev. Lett.* **100**(6) (2008) 063902.
63. X. H. Hong, B. Yang, C. Zhang *et al.*, Nonlinear volume holography for wave-front engineering, *Phys. Rev. Lett.* **113**(16) (2014) 163902.
64. J. Chen and X. Chen, Phase matching in three-dimensional nonlinear photonic crystals, *Phys. Rev. A* **80**(1) (2009) 013801.
65. J. Chen and X. Chen, Generation of conical and spherical second harmonics in three-dimensional nonlinear photonic crystals with radial symmetry, *J. Opt. Soc. Am. B* **28**(2) (2011) 241–246.
66. T. Xu, K. Switkowski, X. Chen *et al.*, Three-dimensional nonlinear photonic crystal in ferroelectric barium calcium titanate, *Nat. Photonic.* **12**(10) (2018) 591.
67. D. Wei, C. Wang, H. Wang *et al.*, Experimental demonstration of a three-dimensional lithium niobate nonlinear photonic crystal, *Nat. Photonic.* **12**(10) (2018) 596.
68. A. Libster-Hershko, S. Trajtenberg-Mills and A. Arie, Dynamic control of light beams in second harmonic generation, *Opt. Lett.* **40**(9) (2015) 1944–1947.
69. I. Dolev, I. Kaminer, A. Shapira *et al.*, Experimental observation of self-accelerating beams in quadratic nonlinear media, *Phys. Rev. Lett.* **108**(11) (2012) 113903.

70. H. Liu, J. Li, X. Zhao *et al.*, Nonlinear Raman-Nath second harmonic generation with structured fundamental wave, *Opt. Exp.* **24**(14) (2016) 15666–15671.
71. H. Zhou, H. Liu, M. Sang *et al.*, Nonlinear Raman-Nath second harmonic generation of hybrid structured fundamental wave, *Opt. Exp.* **25**(4) (2017) 3774–3779.
72. H. Li, H. Liu and X. Chen, Nonlinear vortex beam array generation by spatially modulated fundamental wave, *Opt. Exp.* **25**(23) (2017) 28668–28673.
73. H. Liu, J. Li, X. Fang *et al.*, Dynamic computer-generated nonlinear-optical holograms, *Phys. Rev. A* **96**(2) (2017) 023801.
74. H. Liu, X. Zhao, H. Li *et al.*, Dynamic computer-generated nonlinear optical holograms in a non-collinear second-harmonic generation process, *Opt. Lett.* **43**(14) (2018) 3236–3239.
75. H. Liu, J. Li, X. Fang *et al.*, Scattering-assisted second harmonic generation of structured fundamental wave, *Opt. Exp.* **24**(21) (2016) 24137–24142.
76. X. Fang, H. Liu, X. Zhao *et al.*, Dynamically tailoring nonlinear Cherenkov radiation in PPLN by structured fundamental wave, *J. Nonlinear Opt. Phys. Mater.* **26**(04) (2017) 1750041.
77. B. Yang, X. H. Hong, R. E. Lu *et al.*, 2D wave-front shaping in optical superlattices using nonlinear volume holography, *Opt. Lett.* **41**(13) (2016) 2927–2929.
78. H. Liu, H. Li, Y. Zheng *et al.*, Nonlinear frequency conversion and manipulation of vector beams, *Opt. Lett.* **43**(24) (2018) 5981–5984.